

What can we learn on the thermal history of the Universe from future CMB spectrum measures at long wavelengths?

C. Burigana¹ and R. Salvaterra²

¹*IASF/CNR, Istituto di Astrofisica Spaziale e Fisica Cosmica, Sezione di Bologna, Consiglio Nazionale delle Ricerche, Via Gobetti 101, I-40129 Bologna, Italy*

²*SISSA/ISAS, Astrophysics Sector, Via Beirut, 4, I-34014 Trieste, Italy*

Submitted to MNRAS, 29 December 2002.

ABSTRACT

We analyse the implications of future observations of the CMB absolute temperature at centimeter and decimeter wavelengths, where both ground, balloon and space experiments are currently under study to complement the accurate COBE/FIRAS data available at $\lambda \lesssim 1$ cm.

Our analysis shows that forthcoming ground and balloon measures will allow a better understanding of free-free distortions but will not be able to significantly improve the constraints already provided by the FIRAS data on the possible energy exchanges in the primeval plasma. The same holds even for observations with sensitivities up to ~ 10 times better than those of forthcoming experiments.

Thus, we have studied the impact of very high quality data, such those in principle achievable with a space experiment like DIMES planned to measure the CMB absolute temperature at $0.5 \lesssim \lambda \lesssim 15$ cm with a sensitivity of ~ 0.1 mK, close to that of FIRAS. We have demonstrated that such high quality data would improve by a factor ~ 50 the FIRAS results on the fractional energy exchanges, $\Delta\epsilon/\epsilon_i$, associated to dissipation processes possibly occurred in a wide range of cosmic epochs, at intermediate and high redshifts ($y_h \gtrsim 1$), and that the energy dissipation epoch could be also significantly constrained. By jointly considering two dissipation processes occurring at different epochs, we demonstrated that the sensitivity and frequency coverage of a DIMES-like experiment would allow to accurately recover the epoch and the amount of energy possibly injected in the radiation field at early and intermediate epochs even in presence of a possible late distortion, while the constraints on the energy possibly dissipated at late epochs can be improved by a factor $\simeq 2$. In addition, such measures can provide an independent and very accurate cross-check of FIRAS calibration.

Finally, a DIMES-like experiment will be able to provide indicative independent estimates of the baryon density: the product $\Omega_b H_0^2$ can be recovered within a factor $\sim 2 - 5$ even in the case of (very small) early distortions with $\Delta\epsilon/\epsilon_i \sim (5 - 2) \times 10^{-6}$. On the other hand, for $\Omega_b (H_0/50)^2 \lesssim 0.2$, an independent baryon density determination with an accuracy at \sim per cent level, comparable to that achievable with CMB anisotropy experiments, would require an accuracy of ~ 1 mK or better in the measure of possible early distortions but up to a wavelength from $\sim \text{few} \times \text{dm}$ to ~ 7 dm, according to the baryon density value.

Key words: cosmology: cosmic microwave background – cosmological parameters – cosmology: theory

1 INTRODUCTION

As widely discussed in many papers, the spectrum of the Cosmic Microwave Background (CMB) carries unique informations on physical processes occurring during early cosmic epochs (see e.g. Danese & Burigana 1993 and references therein). The comparison between models of CMB spectral distortions and CMB absolute temperature measures can constrain the physical parameters of the considered dissipation processes. We recently discussed (Salvaterra & Burigana 2002) the implications of the current CMB spectrum data by jointly considering distortions generated in a wide range of early or intermediate cosmic epochs and at late cosmic epochs.

Various CMB spectrum experiments at long wavelengths, $\lambda \gtrsim 1$ cm, are ongoing and planned for the future in order to improve the still quite poor accuracy of the data in this spectral region, where the maximum deviations from a pure blackbody spectrum are expected in the case of dissipation processes occurred at early and intermediate epochs.

In this work we jointly consider the data from the FIRAS instrument aboard the COBE satellite and simulated sets of CMB spectrum observations at wavelengths larger than 1 cm with the sensitivities expected from future experiments in order to discuss their impact for the recovery of the thermal history of the Universe.

In section 2 we briefly summarize the general properties of the CMB spectral distortions and the main physical informations that can be derived from the comparison with the observations. In section 3 we briefly discuss the performances of current and future CMB spectrum observations at long wavelengths and describe the generation of the simulated observations used in this work. The implications of observations with sensitivities typical of forthcoming and future ground and balloon experiments are presented in section 4, while in section 5 we extensively discuss the implications of experiments at long wavelengths with a sensitivity comparable to that of COBE/FIRAS, as foreseen for a space experiment, DIMES, proposed to the NASA in the 1995 and designed to measure the CMB absolute temperature at $\simeq 0.5 - 15$ cm with a sensitivity of ~ 0.1 mK (Kogut 1996). In section 6 we present a detailed discussion of the capabilities of future CMB spectrum observations to discriminate between the FIRAS calibration by the COBE/FIRAS team (referred as here “standard” calibration; see Fixsen et al. 1994, 1996, Mather et al. 1999, and references therein) and that proposed by Battistelli, Fulcoli & Macculi 2000. The possibility to improve our knowledge of the free-free distortions is considered in section 7, while section 8 is devoted to identify the experimental sensitivity requirements for an accurate baryon density evaluation through the detection of possible long wavelength distortions. Finally, we draw our main conclusions in section 9.

2 THEORETICAL FRAMEWORK

The CMB spectrum emerges from the thermalization redshift, $z_{therm} \sim 10^6 - 10^7$, with a shape very close to a Planckian one, owing to the strict coupling between radiation and matter through Compton scattering and photon production/absorption processes, radiative Compton and Bremsstrahlung, which were extremely efficient at early times and able to re-establish a blackbody (BB) spectrum from a perturbed one on timescales much shorter than the expansion time (see e.g. Danese & De Zotti 1977). The value of z_{therm} (Burigana, Danese & De Zotti 1991a) depends on the baryon density (in units of the critical density), Ω_b , and the Hubble constant, H_0 , through the product $\hat{\Omega}_b = \Omega_b (H_0/50)^2$ (H_0 expressed in Km/s/Mpc).

On the other hand, physical processes occurring at redshifts $z < z_{therm}$ may lead imprints on the CMB spectrum.

The timescale for the achievement of kinetic equilibrium between radiation and matter (i.e. the relaxation time for the photon spectrum), t_C , is

$$t_C = t_{\gamma e} \frac{mc^2}{kT_e} \simeq 4.5 \times 10^{28} (T_0/2.7 K)^{-1} \phi^{-1} \hat{\Omega}_b^{-1} (1+z)^{-4} \text{ sec}, \quad (1)$$

where $t_{\gamma e} = 1/(n_e \sigma_{Te})$ is the photon-electron collision time, $\phi = (T_e/T_r)$, T_e being the electron temperature and $T_r = T_0(1+z)$; kT_e/mc^2 is the mean fractional change of photon energy in a scattering of cool photons off hot electrons, i.e. $T_e \gg T_r$; T_0 is the present radiation temperature related to the present radiation energy density by $\epsilon_{r0} = aT_0^4$; a primordial helium abundance of 25% by mass is here assumed.

It is useful to introduce the dimensionless time variable $y_e(z)$ defined by

$$y_e(z) = \int_t^{t_0} \frac{dt}{t_C} = \int_1^{1+z} \frac{d(1+z)}{1+z} \frac{t_{exp}}{t_C}, \quad (2)$$

where t_0 is the present time and t_{exp} is the expansion time given by

$$t_{exp} \simeq 6.3 \times 10^{19} \left(\frac{T_0}{2.7 K} \right)^{-2} (1+z)^{-3/2} \left[\kappa(1+z) + (1+z_{eq}) - \left(\frac{\Omega_{nr} - 1}{\Omega_{nr}} \right) \left(\frac{1+z_{eq}}{1+z} \right) \right]^{-1/2} \text{ sec}, \quad (3)$$

$z_{eq} = 1.0 \times 10^4 (T_0/2.7 K)^{-4} \hat{\Omega}_{nr}$ being the redshift of equal non relativistic matter and photon energy densities (Ω_{nr} is the density of non relativistic matter in units of critical density); $\kappa = 1 + N_\nu(7/8)(4/11)^{4/3}$, N_ν being the number of relativistic,

2-component, neutrino species (for 3 species of massless neutrinos, $\kappa \simeq 1.68$), takes into account the contribution of relativistic neutrinos to the dynamics of the Universe^{*}.

Burigana, De Zotti & Danese 1991b have reported on numerical solutions of the Kompaneets equation (Kompaneets 1956) for a wide range of values of the relevant parameters and accurate analytical representations of these numerical solutions, suggested in part by the general properties of the Kompaneets equation and by its well known asymptotic solutions, have been found (Burigana, De Zotti & Danese 1995).

The CMB distorted spectra depend on at least three main parameters: the fractional amount of energy exchanged between matter and radiation, $\Delta\epsilon/\epsilon_i$, ϵ_i being the radiation energy density before the energy injection, the redshift z_h at which the heating occurs, and the baryon density $\hat{\Omega}_b$. The photon occupation number can be then expressed in the form

$$\eta = \eta(x; \Delta\epsilon/\epsilon_i, y_h, \hat{\Omega}_b), \quad (4)$$

where x is the dimensionless frequency $x = h\nu/kT_0$ (ν being the present frequency), and $y_h \equiv y_e(z_h)$ characterizes the epoch when the energy dissipation occurred, z_h being the corresponding redshift (we will refer to $y_h \equiv y_e(z_h)$ computed assuming $\phi = 1$, so that the epoch considered for the energy dissipation does not depend on the amount of released energy). The continuous behaviour of the distorted spectral shape with y_h can be in principle used also to search for constraints on the epoch of the energy exchange. Of course, by combining the approximations describing the distorted spectrum at early and intermediate epochs with the Comptonization distortion expression describing late distortions, it is possible to jointly treat two heating processes (see Burigana et al. 1995 and Salvaterra & Burigana 2002 and references therein for a more exhaustive discussion).

In this work the measures of the CMB absolute temperature are compared with the above models of distorted spectra for one or two heating processes by using a standard χ^2 analysis.

We determine the limits on the amount of energy possibly injected in the cosmic background at arbitrary primordial epochs corresponding to a redshift z_h (or equivalently to y_h). This topic has been discussed in several works (see e.g. Burigana et al. 1991b, Nordberg & Smoot 1998, Salvaterra & Burigana 2002). As in Salvaterra & Burigana 2002, we improve here the previous methods of analysis by investigating the possibility of properly combining FIRAS data with longer wavelength measures with the sensitivities expected for forthcoming and future experiments and by refining the method of comparison with the theoretical models. We will consider the recent improvement in the calibration of the FIRAS data, that sets the CMB scale temperature at 2.725 ± 0.002 K at 95 per cent confidence level (CL) (Mather et al. 1999). We do not consider the effect on the estimate of the amount of energy injected in the CMB at a given epoch introduced by the calibration uncertainty of FIRAS scale temperature when FIRAS data are treated jointly to longer wavelength measures, since the analysis of Salvaterra & Burigana 2002 shows that it introduces only minor effects.

Then, we study the combined effect of two different heating processes that may have distorted the CMB spectrum at different epochs. This hypothesis has been also taken into account by Nordberg & Smoot 1998, who fit the observed data with a spectrum distorted by a single heating at $y_h = 5$, a second one at $y_h \ll 1$ and by free-free emission, obtaining limits on the parameters that describe these processes. As in Salvaterra & Burigana 2002, we extend their analysis by considering the full range of epochs for the early and intermediate energy injection process, by taking advantage of the analytical representation of spectral distortions at intermediate redshifts (Burigana et al. 1995). Since the relationship between free-free distortion and Comptonization distortion is highly model dependent, being related to the details of the thermal history at late epochs (Danese & Burigana 1993, Burigana et al. 1995), and can not be simply represented by integral parameters, we avoid a combined analysis of free-free distortions and other kinds of spectral distortions and separately discuss the implications of future, more accurate long wavelength measures on free-free distortions.

It is also possible to extend the limits on $\Delta\epsilon/\epsilon_i$ for heatings occurred at $z_h > z_1$, where z_1 is the redshift corresponding to $y_h = 5$, when the Compton scattering was able to restore the kinetic equilibrium between matter and radiation on timescales much shorter than the expansion time and the evolution on the CMB spectrum can be easily studied by replacing the full Kompaneets equation with the differential equations for the evolution of the electron temperature and the chemical potential. This study can be performed by using the simple analytical expressions by Burigana et al. 1991b instead of numerical solutions.

A recent analysis of the limits on the amount of the energy possibly injected in the cosmic background from the currently available data is reported in Salvaterra & Burigana 2002. In particular, they found that the measures at $\lambda \gtrsim 1$ cm do not significantly contribute to these constraints because of their poor sensitivity compared to that of FIRAS. New and more accurate measurements are also needed in this range, which is particular sensitive to early energy injection processes. In fact, the current constraints on $\Delta\epsilon/\epsilon_i$ at $y_h \sim 5$ are a factor ~ 2 less stringent than those at y_h less than ~ 0.1 , because of the frequency coverage of FIRAS, which mainly set the current constraints at the all cosmic epochs. Thus, we are interested to investigate the role of future ground, balloon and space experiments at $\lambda \gtrsim 1$ cm jointed to the FIRAS measures at $\lambda \lesssim 1$ cm.

^{*} Strictly speaking the present ratio of neutrino to photon energy densities, and hence the value of κ , is itself a function of the amount of energy dissipated. The effect, however, is never very important and is negligible for very small distortions.

To evaluate the scientific impact represented by the future experiment improvements, we create different data sets simulating the observation of a not distorted spectrum both from ground and balloon experiments and from a space experiment like DIMES through the method described in section 3.1. For a DIMES-like experiment, we also explore the possibility of the observation of distorted spectra for different amounts of the energy injected in the radiation field and for different cosmic epochs.

Each data set will be then compared to models of distorted spectra by using the method described in Salvaterra & Burigana 2002 (see also Burigana & Salvaterra 2000 for the details of the code) to recover the value of $\Delta\epsilon/\epsilon_i$ or constraints on it, the heating epoch, y_h , the free-free distortion parameter y_B , and the combination, $\hat{\Omega}_b$, of the baryon density and the Hubble constant.

For simplicity, we restrict to the case of a baryon density $\hat{\Omega}_b = 0.05$ our analysis of the implications for the thermal history of the Universe, but the method can be simply applied to different values of $\hat{\Omega}_b$. In presence of an early distortion, $\hat{\Omega}_b$ could be in principle measured by CMB spectrum observations at long wavelengths provided that they have the required sensitivity about the minimum of the CMB absolute temperature (see section 8).

3 FUTURE EXPERIMENTS

The CMB spectrum experiments currently under study are dedicated to improve our knowledge at wavelengths longer than those covered by FIRAS. At centimeter and decimeter wavelengths, the available measures typically show large error bars although some experiments are rather accurate (i.e., the measure of Staggs et al. 1996 at $\simeq 2.8$ cm). Very accurate data at long wavelengths could give a significant improvement to our knowledge of physical processes in the primeval plasma, particularly at high redshifts. These projects regard measurements from ground, balloon and space. As representative cases, and without the ambition to cover the whole set of planned experiments, we briefly refer here to the ground experiment TRIS at very long wavelengths and to the DIMES experiment from space (Kogut 1996) designed to reach an accuracy close to that of FIRAS up to $\lambda \simeq 15$ cm.

TRIS[†] is a set of total power radiometers designed to measure the absolute temperature of the CMB at three frequencies: 0.6, 0.82 and 2.5 GHz.

At these wavelengths (12 – 50 cm) the measurements are difficult because the CMB signal is comparable to other components of the antenna temperature: Galactic background, unresolved extra-galactic sources, sidelobes pickup and atmospheric emission. To improve the experimental situation, TRIS will make absolute maps of large areas of the sky at the three frequencies, to disentangle the various components of the celestial signal; all the lossy parts of the antenna front ends of the receivers will be cooled down liquid helium temperature, to reduce the thermal noise of these components; the receiver temperatures will be very carefully stabilized to reduce drifts and gain variations. The TRIS expected sensitivity is of about 200 mK at the three frequencies.

DIMES[‡] (Diffuse Microwave Emission Survey) is a space mission submitted to the NASA in 1995, designed to measure very accurately the CMB spectrum at wavelengths in the range $\simeq 0.5 - 15$ cm (Kogut 1996).

DIMES will compare the spectrum of each 10 degree pixel on the sky to a precisely known blackbody to precision of ~ 0.1 mK, close to that of FIRAS ($\simeq 0.02 - 0.2$ mK). The set of receivers is given from cryogenic radiometers operating at six frequency bands about 2, 4, 6, 10 e 90 GHz using a single external blackbody calibration target common to all channels. In each channel, a cryogenic radiometer switched for gain stability between an internal reference load and an antenna with 10 degree beam width, will measure the signal change as the antenna alternately views the sky and an external blackbody calibration target. The target temperature will be adjusted to match the sky signal in the lowest frequency band, allowing the absolute temperature to be read off from the target thermometry with minimal corrections for the instrumental signature. With its temperature held constant, the target will rapidly move over the higher-frequencies antenna apertures, effectively comparing the spectrum of diffuse emission from the sky to a precise blackbody. By comparing each channel to the same target, uncertainties in the target emission cancel so that deviations from a blackbody spectral shape may be determined much more precisely than the absolute temperature. The DIMES design is driven by the need to reduce or eliminate systematic errors from instrumental artifacts. The instrument emission will be cooled to 2.7 K, whereas the calibration uncertainty will be minimized by using a single calibration target, common to all channels. The atmospheric emission will be observed from low Earth orbit and the multiple channels measurements will minimize the foreground emission problems. The DIMES sensitivity represents an improvement by a factor better than 300 with respect to previous measurements at cm wavelengths.

[†] <http://sunradio.uni.mi.astro.it/grupporadio/tris/index.html>

[‡] <http://map.gsfc.nasa.gov/DIMES/index.html>

3.1 Generation of simulated data sets

We collect different data sets, simulating measurements of different CMB spectra, distorted or not, at the frequency ranges of the considered experiments. We add to these simulated data the FIRAS data at higher frequencies according to the most recent calibration of the temperature scale at 2.725 K (Mather et al. 1999).

For the cases of distorted spectra we calculate the theoretical temperature of the CMB spectrum at the wavelengths of the new experiments as discussed in the previous section. Of course, the thermodynamic temperature held obviously constant at all the frequencies for the case of a non distorted spectrum.

The theoretical temperatures are then fouled to simulate real measurements affected by instrumental noise. The simulated temperature T_{obs} at the frequency ν is given by

$$T_{obs}(\nu) = T_{teor}(\nu) + n(\nu) \times \text{err}(\nu), \quad (5)$$

where $T_{teor}(\nu)$ is the theoretical temperature at the frequency ν and $\text{err}(\nu)$ is the expected rms error (at 1σ) of the experiment at this frequency. The numbers n are a set of random numbers generated according to a Gaussian distribution with null mean value and unit variance with the routine GASDEV by Press et al. 1992 (§7).

4 IMPLICATIONS OF FUTURE GROUND AND BALLOON EXPERIMENTS

We analyse here the impact of possible future observations from ground and balloon in the case of a not distorted spectrum at the temperature $T_0 = 2.725$ K. The results are thus comparable to those obtained with the FIRAS data alone (see e.g. Salvaterra & Burigana 2002).

4.1 Simulated data sets

To build the first simulated data set (G&B1-BB), we split the region from 1 to 80 cm in three ranges and associate different values of sensitivity to each range according to the analysis of the main problems affecting the available observations in different spectral regions (e.g. Salvaterra & Burigana 2000).

(i) 1 – 4 cm. In this range the measurements of Staggs et al. 1996 show an uncertainty of ~ 40 mK. Thus, quite accurate measures could be carried out in this range. We choose to associate to the future experiments at these wavelengths an improved typical sensitivity of 10 mK.

(ii) 4 – 9 cm. Ground experiments in this range show error bars of about 50 – 70 mK. Progresses could be reached by improving the accuracy of the subtraction of the atmospheric contribution which dominates the final error at these wavelengths. Thus, we choose to associate to the data in this region a typical sensitivity of 40 mK;

(iii) 10 – 80 cm. Observations in this range are still quite difficult, the typical sensitivities being between 200 mK for measures at 10 cm and 1.5 K for those at longer wavelengths. The expected sensitivity of the TRIS experiment (see section 3) is of ~ 200 mK. Thus, we choose to associate to future experiments in this range a typical sensitivity of 200 mK.

The frequencies of the experiments at $\lambda \gtrsim 1$ cm of the two last decades (see e.g. Table 1 of Salvaterra & Burigana 2002), where suitable observation windows should exist and the presence of man made interferences should be not a concern, have been adopted in the generation of simulated observations.

Finally, we complete this data set by adding the FIRAS measures calibrated at 2.725 K according to Mather et al. 1999 to the above simulated data.

A second data set (G&B2-BB) is built as before but by improving by a factor 10 the sensitivity associated to each of the above three frequency range in order to evaluate the impact of highly optimistic future progresses of ground and ballon experiments.

4.2 Fits to simulated data

The results of the fits to the simulated data G&B1-BB and G&B2-BB jointed to FIRAS data are shown in Fig. 1 [for graphic purposes, we report in the plots the exact value of y_h and the power-law approximation $z_h(y_h) \simeq 4.94^4 y_h^{0.477} \widehat{\Omega}_b^{-0.473}$ (Burigana et al. 1991b) for the redshift]. As evident, realistic improvements of future experiments from ground and balloon do not significantly change the FIRAS limits. Even under much more optimistic experimental conditions, able to decrease the errors by a factor 10, the situation can not substantially improve, being the limits on $\Delta\epsilon/\epsilon_i$ obtained in this case only just more stringent than those based on FIRAS data alone.

We then conclude that, unfortunately, observations of the CMB absolute temperature with sensitivity levels typical of future ground and balloon experiments do not seem able to improve the limits on the amount of energy injected in the cosmic radiation field inferred on the basis of the currently available measures.

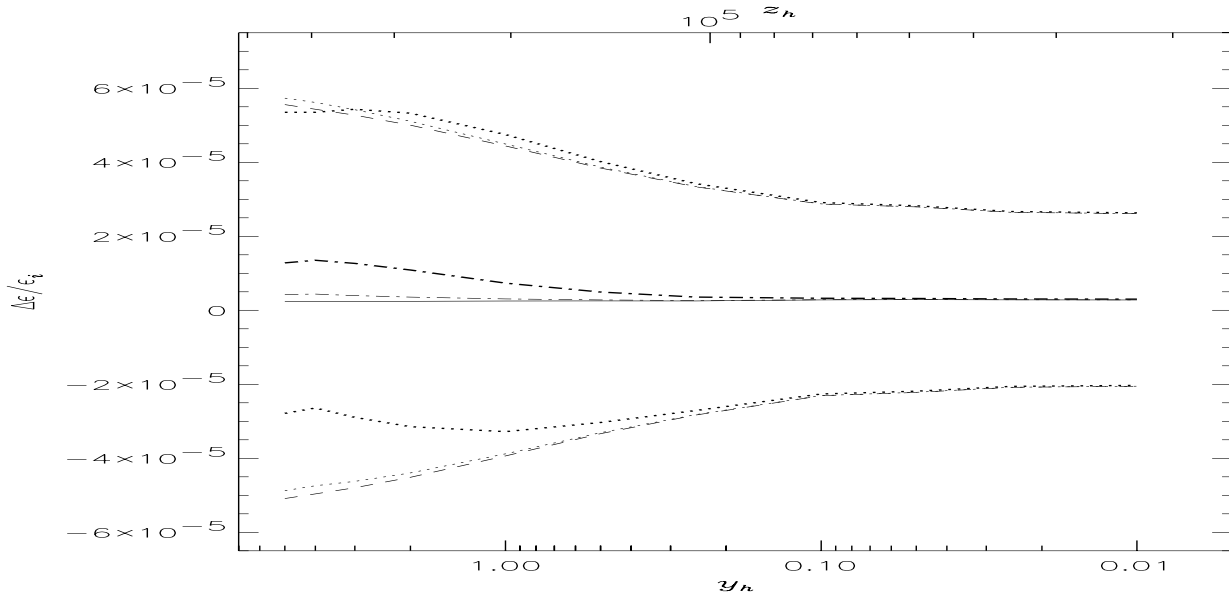


Figure 1. Comparison between the constraints (at 95 per cent CL) on the energy exchanges derived at different cosmic times from different data sets by considering the case of a single dissipation process. The different lines refer to: FIRAS data calibrated according to Mather et al. 1999 (solid line: best fit; dashed lines: upper and lower limits); FIRAS data jointed to the data set G&B1-BB (dot-dashes: best fit; dots: upper and lower limits); FIRAS data jointed to the data set G&B2-BB (thick dot-dashes: best fit; thick dots: upper and lower limits).

5 IMPLICATIONS OF A DIMES-LIKE EXPERIMENT

5.1 Simulated data sets

We generate a set (D-BB) of simulated data in the case of a blackbody spectrum at a temperature of 2.725 K in order to evaluate the capability of an experiment with a sensitivity comparable to that expected for DIMES to improve the constraints on the amount of the energy injected in the cosmic radiation field. The analysis of this case is in fact directly comparable with the results obtained from the fit to the FIRAS data alone.

Then, we build up other data sets representing the observations of CMB spectra distorted by energy injections at different cosmic epochs in order to investigate the possibility of a DIMES-like experiment to firmly determine the presence of spectral distortions. We consider processes occurring at a wide range of cosmic epochs, represented by the dimensionless time $y_h = 5, 4, 3, 2, 1, 0.5, 0.25, 0.1, 0.05, 0.025, 0.01$, and $y_h \ll 1$. We consider four representative values of fractional injected energy: $\Delta\epsilon/\epsilon_i = 2 \times 10^{-5}$, a value not much below the upper FIRAS limits; $\Delta\epsilon/\epsilon_i = 2 \times 10^{-4}$, well above the FIRAS upper limit (see section 6); $\Delta\epsilon/\epsilon_i = 5 \times 10^{-6}$ and 2×10^{-6} , two values well below the FIRAS upper limit, to test the chances to detect very small distortions with a DIMES-like experiment.

As a further representative case, we simulate the observation of a spectrum distorted by two heating processes occurring at different epochs, the first at $y_h = 5$ and the second at $y_h \ll 1$, both characterized by $\Delta\epsilon/\epsilon_i = 5 \times 10^{-6}$.

All these distorted spectra are computed by setting $\Omega_b = 0.05$ and $H_0 = 50$ Km/s/Mpc.

As a variance with respect to the previous section, we choose here the frequencies of the simulated observations by adopting the five frequency channels of the DIMES experiment.

As in previous section, we complete these data set by adding the FIRAS measures calibrated at 2.725 K.

5.2 Fits to simulated data: analysis of a single dissipation process

5.2.1 Non distorted spectrum

We fit the simulated data D-BB with a spectrum distorted by an energy injection at different values of y_h in order to recover the value of $\Delta\epsilon/\epsilon_i$, expected to be null, and the limits on it. The fit results are reported in Fig. 2.

It is evident how future data at this sensitivity level will allow a strong improvement of the limits obtained with the FIRAS data alone. The recovered best-fit value of $\Delta\epsilon/\epsilon_i$ is always compatible with the absence of distortions within the limits at 95 per cent CL. For heating processes at low z ($y_h = 0.1 - 0.01$) the fit is substantially dominated by the FIRAS data and the lower and the upper limits on $\Delta\epsilon/\epsilon_i$ are still $\sim 2 \times 10^{-5}$. On the contrary, for early distortions ($y_h \gtrsim 1$) the low frequency measures of a DIMES-like experiment will allow to improve the FIRAS constraints by a factor $\sim 10 - 50$, the proper

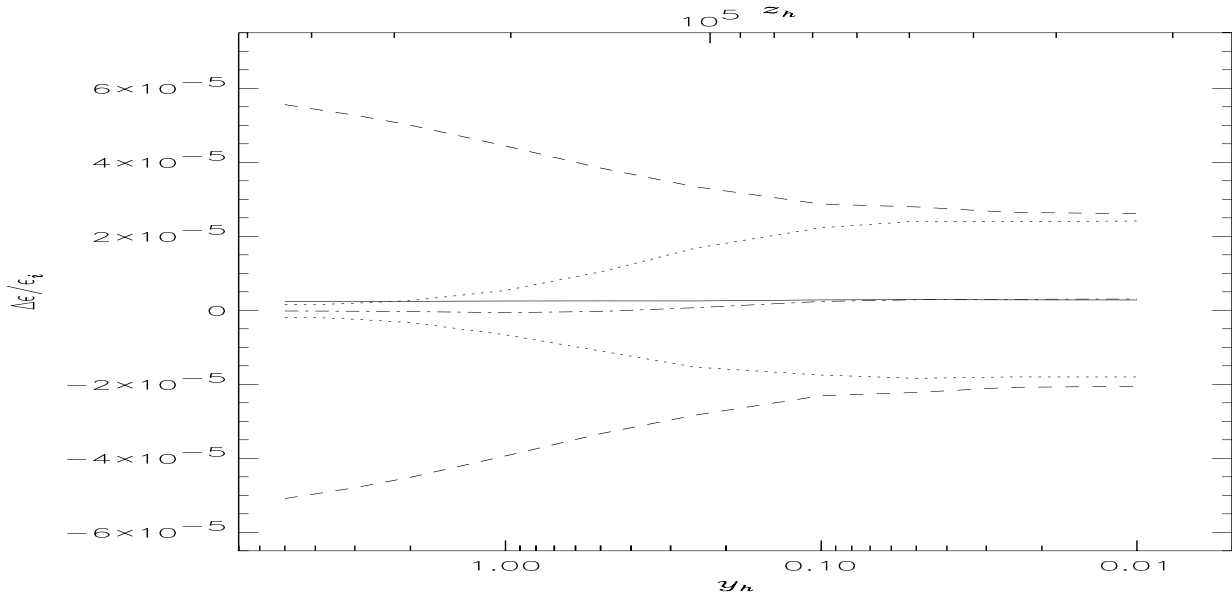


Figure 2. Comparison between the constraints (at 95 per cent CL) on the energy exchanges derived at different cosmic times from different data sets by considering the case of a single dissipation process. The different lines refer to: FIRAS data calibrated according to Mather et al. 1999 (solid line: best fit; dashed lines: upper and lower limits); FIRAS data jointed to the data set D-BB (dot-dashes: best fit; dots: upper and lower limits).

value increasing with the considered dissipation redshift. We conclude that measures from an instrument like DIMES could represent a very good complement to the FIRAS data.

In the next sections we will analyse in detail the capability of a DIMES-like experiment to determine the presence of spectral distortions possibly present in the CMB spectrum.

5.2.2 Distorted spectra

The test reported in the previous section suggests that even small distortions could be determined provided that the dissipation would have occurred at relatively early epochs, $y_h \gtrsim 1$. Thus, we analyse the sensitivity of a DIMES-like experiment in the recovery of the amount of energy possibly injected in the radiation field and explore also the possibility to determine the dissipation process epoch.

Firstly, we fit the data simulated as above under the hypothesis that the heating epoch is known; more explicitly, we fit the data with a theoretical spectrum distorted by a process occurring at the considered y_h by allowing to optimize $\Delta\epsilon/\epsilon_i$ (and T_0) but by taking y_h fixed. In this way we can see how accurately $\Delta\epsilon/\epsilon_i$ could be in principle recovered.

On the other hand, unless we want to use the CMB spectrum data to constrain theoretical models with a well defined dissipation epoch, we are typically interested to set constraints on the value of $\Delta\epsilon/\epsilon_i$ possibly injected at a given unknown epoch occurring within a relatively wide cosmic period; in addition, many classes of physical processes in the plasma epoch involve time parameters and it is important to understand how they can be possibly constrained by the comparison with CMB spectrum observations.

Thus, we focus on the cases of spectra distorted at high ($y_h = 5$), medium ($y_h = 1.5$) and at low ($y_h \ll 1$) redshifts by fitting the simulated data by relaxing the a priori knowledge of the dissipation epoch. In this way we would be able to evaluate the possibility of determining also the epoch of the heating [§] without a priori informations by jointly evaluating the impact of the unknowledge of the dissipation epoch on the recovery of injected energy. We will test also the possibility of deriving at the same time information on the baryon density.

5.2.2.1 Energy injections at FIRAS limits – Dissipation epoch: known

As a representative case we consider the simulated observation of a spectrum distorted at different values of y_h by an energy injection with $\Delta\epsilon/\epsilon_i = 2 \times 10^{-5}$, a value below, but not much, the FIRAS upper limit on $\Delta\epsilon/\epsilon_i$. These data are then compared

[§] Of course, any energy injection occurred at a certain $y_h > 5$ with a proper higher value of $\Delta\epsilon/\epsilon_i$ would give a distorted spectrum essentially indistinguishable by that generated in the case of a dissipation at $y_h = 5$ with a lower value of $\Delta\epsilon/\epsilon_i$, see section 5.4.

with the theoretical CMB spectrum distorted at the same y_h (assumed to be known) by performing the fit only over $\Delta\epsilon/\epsilon_i$ and T_0 : this is appropriate to cases in which we have a quite well defined a priori information on the dissipation epoch but not on the amount of released energy.

We find that for high redshift processes, $y_h \simeq 2 - 5$, $\Delta\epsilon/\epsilon_i$ is precisely determined. For distortions at lower z , $y_h \lesssim 1$, we obtain limits similar to those given from the currently available data, since the fit result is mainly driven by FIRAS data, more sensitive to these kinds of distortions, mainly located at high frequencies.

5.2.2.2 Energy injections at FIRAS limits – Dissipation epoch: unknown

We relax here the assumption to know the dissipation epoch. We consider firstly the case of the fit to data simulated assuming a spectrum distorted at $y_h = 5$ with $\Delta\epsilon/\epsilon_i = 2 \times 10^{-5}$ with CMB theoretical spectra distorted at different values of y_h . The best-fit to these data assuming $y_h = 5$ gives a very accurate recovery of the input value of $\Delta\epsilon/\epsilon_i$ with a small quoted error (we find an associated statistical error of $\simeq 10\%$ at 95 per cent CL). The best-fit on $\Delta\epsilon/\epsilon_i$ assuming lower values of y_h is far from the input value and the χ^2 increases. Thus, we search for a favourite value of y_h by performing the fit over $\Delta\epsilon/\epsilon_i$, T_0 , and y_h . We obtain that the recovered best-fit value of y_h is exactly the input one, 5.0, and lower limit on y_h at 95 per cent CL is 2.4. By searching also for a favourite value of $\hat{\Omega}_b$ (set to 0.05 in the data simulation), we obtain a 68 per cent CL range of $\simeq 0.01 - 0.096$.

We repeated the same analysis in the case of a spectrum distorted at $y_h = 1.5$ with $\Delta\epsilon/\epsilon_i = 2 \times 10^{-5}$. Again, the recovered value of $\Delta\epsilon/\epsilon_i$ is close to the input one for fits with $y_h \simeq 1.5$ (in this case we recover the input value of $\Delta\epsilon/\epsilon_i$ with an uncertainty of $\simeq 18\%$ at 95 per cent CL) and we are also able to determine a significative range ($y_h \gtrsim 1$ at 95 per cent CL) of favourite values of y_h , although wider than in the previous case, while $\hat{\Omega}_b$ is found to be in the range $\simeq 0.024 - 0.091$ at 68 per cent CL.

Similar results on y_h and $\hat{\Omega}_b$ can not be obtained in the case of fit to the data simulating the observation of a spectrum distorted at $y_h \sim 0.01$. The fit result then is then compatible also with energy injections with smaller values of $\Delta\epsilon/\epsilon_i$ but at higher y_h and with a non distorted spectrum. The χ^2 value does not significantly change when y_h varies. This is again the result of the main role of FIRAS data for late dissipation processes.

5.2.2.3 Energy injections below FIRAS limits – Dissipation epoch: known

A DIMES-like experiment should be able to detect also small spectral distortions. Let consider here the case of a spectrum distorted from an energy injection with $\Delta\epsilon/\epsilon_i = 5 \times 10^{-6}$, about a factor 10 below the FIRAS limits at 95 per cent CL.

As shown in Fig. 3, if the dissipation epoch is known, we find that for processes at early and intermediate epochs the best-fit result is very close to the input value of the simulated data, although the limits on $\Delta\epsilon/\epsilon_i$ are not so stringent as in the case with a larger energy injection. For $y_h \gtrsim 1$, a spectral distortion would be firmly detected at 95 per cent CL.

5.2.2.4 Energy injections below FIRAS limits – Dissipation epoch: unknown

We relax here again the assumption to know the dissipation epoch. Our results are summarized in Fig. 4: even for distortions well below the FIRAS limits ($\Delta\epsilon/\epsilon_i = 5 \times 10^{-6}$ is assumed here) an experiment like DIMES would provide significative constraints both on the amount of dissipated energy and on the dissipation epoch in the case of and early processes. In this test the input dissipation epoch ($y_h = 5$) is again quite well recovered, the χ^2 increasing of 4 when y_h becomes close to unity. It would be also possible to provide an independent estimate of the baryon density: we find $\hat{\Omega}_b \simeq 0.01 - 0.18$ at 68 per cent CL.

For a process occurring at intermediate epochs ($y_h = 1.5$ in this specific test) we find that it is still possible to determine the amount of injected energy, but in this case of distortions significantly smaller than the FIRAS limits the χ^2 is no longer particularly sensitive to y_h and the recovered range of dissipation epochs is wide. Energy dissipations processes at intermediate epochs may then result still compatible with these simulated data and only energy injections at late epochs, could be excluded (in this test we find that the χ^2 increases of $\simeq 4$ for $y_h \simeq 0.1$).

As already found for larger distortions, significant information on late processes can not be obtained from accurate long wavelength data because of the more relevant role of the FIRAS data.

5.2.2.5 Very small energy injections

Finally, we consider the possibility to detect very small energy injections, namely with $\Delta\epsilon/\epsilon_i = 2 \times 10^{-6}$.

If the dissipation epoch is known, the result of the fit shows that is still possible to determine a no null distortion provided that the dissipation process occurs at high redshifts.

For energy injections at epochs close to $y_h = 5$ the recovered value of $\Delta\epsilon/\epsilon_i$, $\simeq 2.5 \times 10^{-6}$ in this test, is quite close to the input one and the associate statistical error gives a $\Delta\epsilon/\epsilon_i$ range of $\simeq (1 - 4.5) \times 10^{-6}$ at 95 per cent CL. An indication of

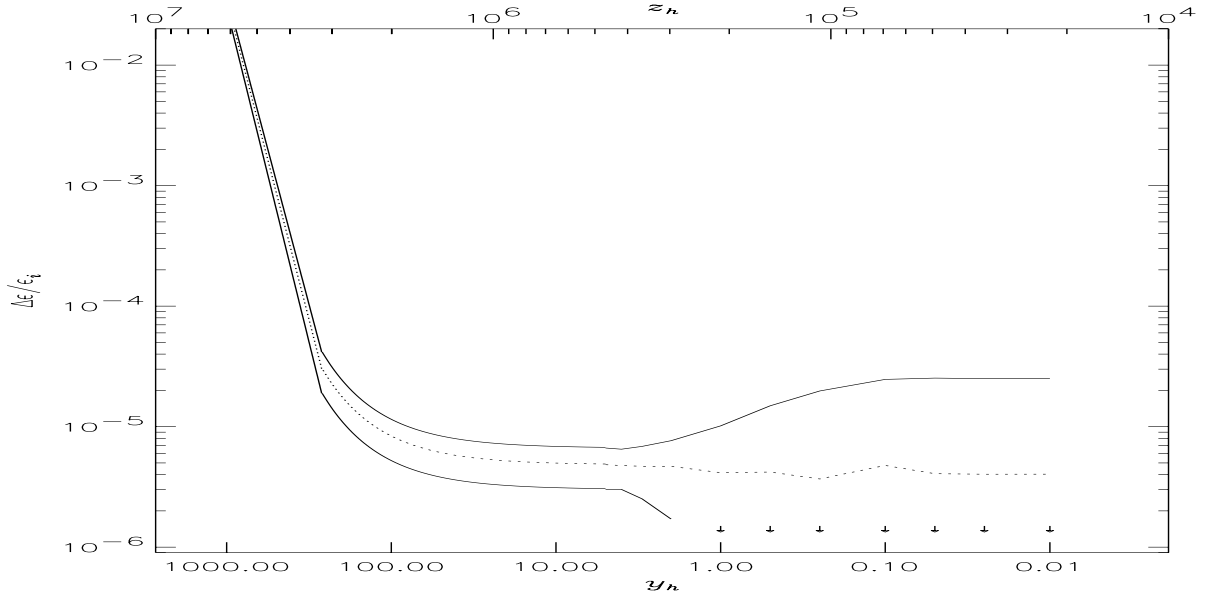


Figure 3. Constraints on the energy exchanges derived at different cosmic times by considering the case of a single dissipation process on the basis of the FIRAS data calibrated according to Mather et al. 1999 and data simulated as in the case of an energy injection with $\Delta\epsilon/\epsilon_i \geq 5 \times 10^{-6}$ and observed with a DIMES-like experiment. The dissipation epoch is assumed to be known (is the same in the generation of simulated data and in the fit). The different lines refer to the best fit result (dots) and to the upper and lower limits at 95 per cent CL (solid lines). The arrows indicate that the sign of the lower limit changes at $y_h \simeq 1$, where lower and upper error bars result to be very similar.

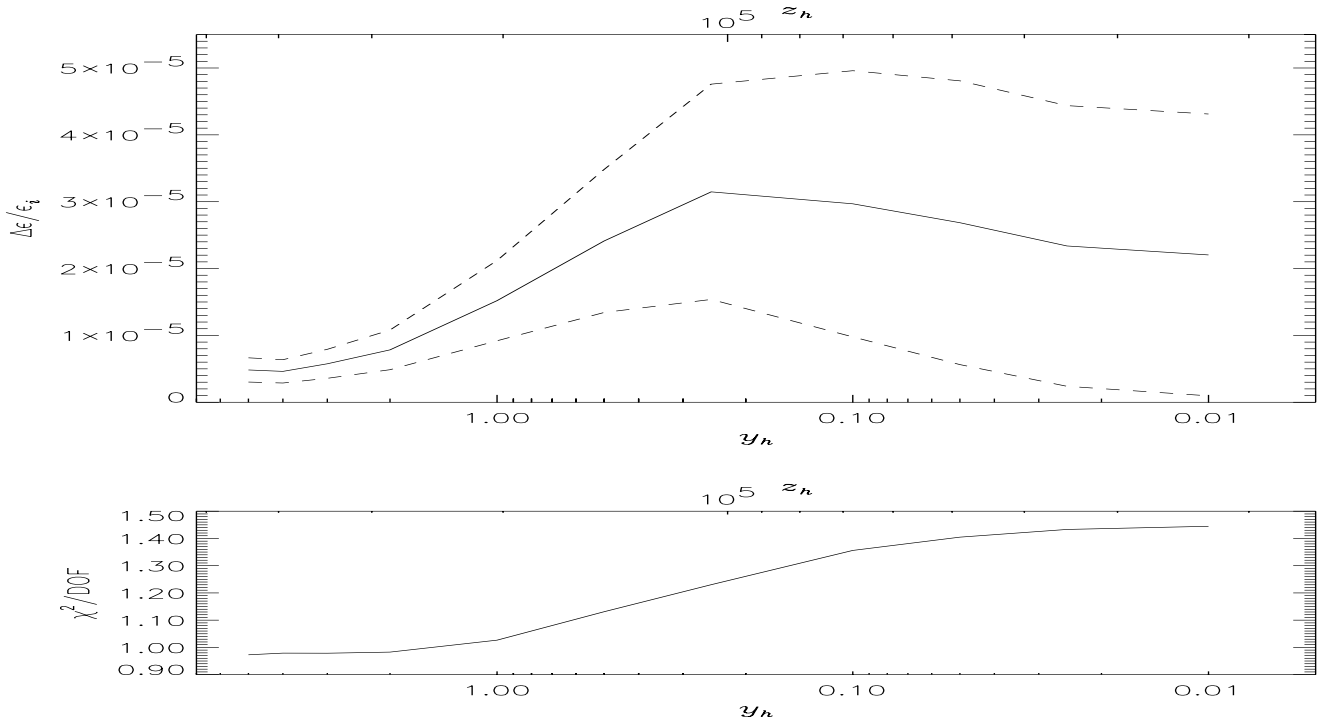


Figure 4. Constraints on the energy exchanges derived at different cosmic times by considering the case of a single dissipation process on the basis of the FIRAS data calibrated according to Mather et al. 1999 and data simulated as in the case of an energy injection with $\Delta\epsilon/\epsilon_i \geq 5 \times 10^{-6}$ occurring at $y_h = 5$ and observed with a DIMES-like experiment (top panel). The different lines refer to the best fit result (solid line) and to the upper and lower limits at 95 per cent CL (dashes) by assuming a dissipation process occurring at a given value of y_h . Note that the $\chi^2/\text{d.o.f.}$ increases for decreasing y_h , i.e. when the dissipation epoch assumed in the fit is different from that adopted in the generation of the simulated data (bottom panel): this implies that a DIMES-like experiment could provide interesting constraints also on the epoch of a possible energy exchange.

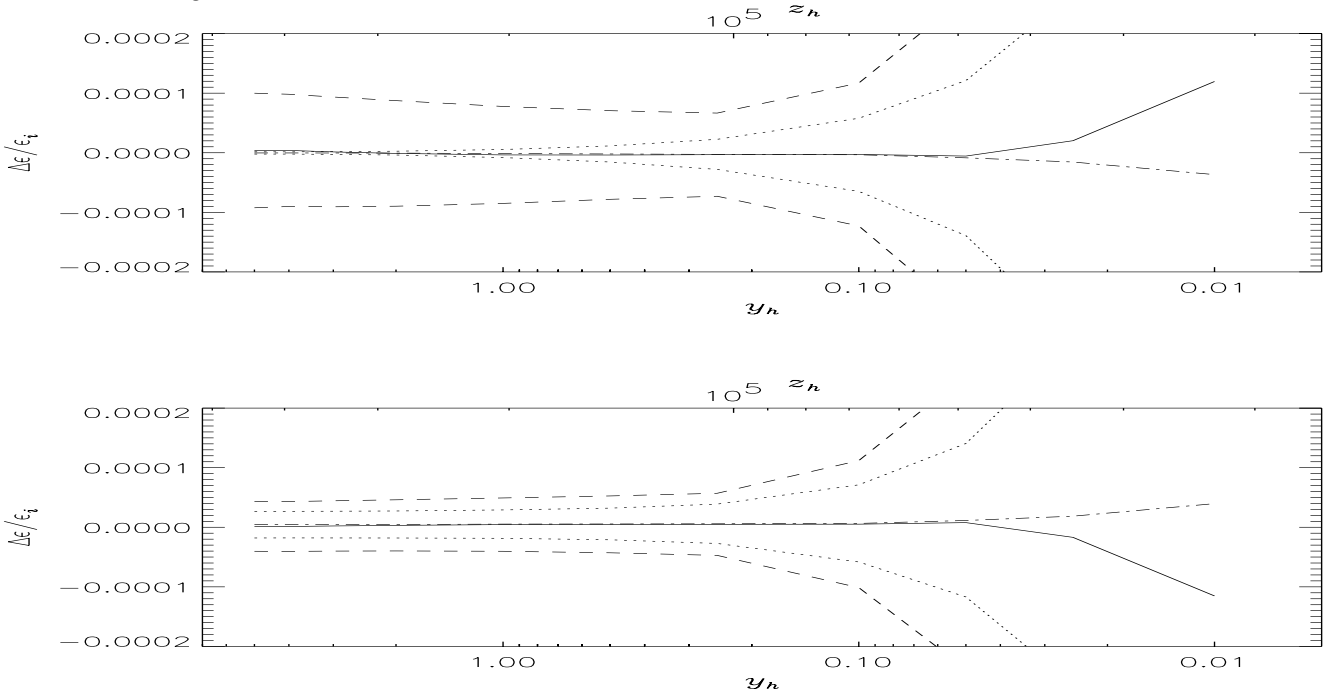


Figure 5. Constraints at 95 per cent CL on the energy exchanges derived from current measures, FIRAS and long wavelength data (in practice FIRAS data alone set the current constraints, see Salvaterra & Burigana 2002; solid lines: best fit; dashes: upper and lower limits) and from FIRAS data jointed to the simulated data set D-BB (dash-dotted line: best fit; dots: upper and lower limits). The top panel refers to the constraints on early/intermediate energy exchanges occurring at the considered y_h obtained by allowing for a possible late dissipation process. The bottom panel refers to the constraints on late energy exchanges obtained by allowing for a possible dissipation process at an early/intermediate epoch occurring at the considered y_h . Note the large improvement (up to a factor $\simeq 50$) of the constraints on early/intermediate processes, because of the long wavelength coverage of DIMES-like experiment, and that also the constraints on processes at late epochs could improve (by a factor $\simeq 2$). See also the text.

the dissipation epoch can be also derived (in this case we find that the χ^2 increases of $\simeq 4$ for $y_h \simeq 0.5$). Unfortunately, no significant informations on $\hat{\Omega}_b$ can be obtained with the considered sensitivity and frequency coverage in the case of so small distortions.

For dissipations at $y_h \sim 1.5$ a significative distortion can be also determined, the recovered value of $\Delta\epsilon/\epsilon_i$ ranging between $\simeq 0$ and $\sim 8 \times 10^{-6}$ at 95 per cent CL for $y_h \sim 1 - 2$ where the $\chi^2/\text{d.o.f.}$ is about its minimum, but significative informations on the dissipation epoch can be no longer derived.

Finally, in the case of processes at late epochs, the fit results are compatible with an unperturbed spectrum, being these kind of distortions mainly detectable at FIRAS frequencies.

5.3 Fits to simulated data: joint analysis of two dissipation processes

We discuss here the possibility to significantly improve the constraints on (or to detect) energy exchanges also in the more general case of a joint analysis of early/intermediate and late dissipation processes.

5.3.1 Non distorted spectrum

By exploiting the data set D-BB presented in Sect. 5.1 we consider the case of no significant deviations from a Planckian spectrum. Top panel of Fig. 5 shows the limits on the energy exchange as function of y_h by allowing for a later dissipation process possibly occurred at $y_h \ll 1$; bottom panel of Fig. 5 shows the constraints on the energy injected at low z by allowing for a previous distortion occurred at any given y_h . In Fig. 5 we report also the comparison with the results based only on the FIRAS data (as shown in Salvaterra & Burigana 2002, the current long wavelength measures do not change significantly these results). The conclusion is impressive: the constraints on $\Delta\epsilon/\epsilon_i$ for early and intermediate dissipation processes could be improved by a factor $\simeq 10 - 50$, depending on the considered dissipation epoch. In addition, the constraints on the energy dissipation at late epochs can be also improved, by a factor of about two, because of the reduction of the partial degeneracy introduced by the rough compensation (Salvaterra & Burigana 2002) between the effect of early and late energy exchanges on the CMB spectrum when no accurate measures are available at long wavelengths.

5.3.2 Distorted spectra

To complete the analysis of the impact of a possible DIMES-like experiment, we consider the simulated observation of a spectrum distorted by a first energy dissipation at $y_h = 5$ with $\Delta\epsilon/\epsilon_i = 5 \times 10^{-6}$ and a second one at $y_h \ll 1$ with $\Delta\epsilon/\epsilon_i = 5 \times 10^{-6}$. We then compare these data with theoretical spectra distorted by a process at $y_h \ll 1$ and another at any given $y_h \lesssim 5$ according to our grid of y_h (see section 5.1).

We find that a DIMES-like experiment would allow to firmly determine the presence of the distortion at high z ; in particular, at $y_h = 5$ the recovered $\Delta\epsilon/\epsilon_i$ is very close to the input one, as already found for the tests described in sections 5.2.2.3 and 5.2.2.4. On the contrary, for the dissipation process at $y_h \ll 1$ the fit result is compatible with an unperturbed spectrum, since the FIRAS data dominate the limits on the distortions at low redshifts. The limits on $\Delta\epsilon/\epsilon_i$ for processes at low redshifts are, however, again more stringent, by a factor 2, than those obtained with the currently available data.

We find that the χ^2 significantly increases by assuming in the fit an earlier process at decreasing y_h (the χ^2 increases of $\simeq 4$ for $y_h \simeq 1$): even in the case of a combination of an early and a late process a DIMES-like experiment would be able to significantly constrain the epoch of the earlier energy exchange.

5.4 Constraints on very high redshift processes

We extend here at $z_h > z_1$ (i.e. $y_h > 5$) the constraints on $\Delta\epsilon/\epsilon_i$ that would be possible to derive at $z_h = z_1$ ($y_h = 5$) with a DIMES-like experiment. We remember that at $z > z_1$ the Compton scattering is able to restore, after an energy injection, the kinetic equilibrium between matter and radiation, yielding a Bose-Einstein (BE) spectrum, and the combined effect of Compton scattering and photon production processes tends to reduce the magnitude of spectral distortions, possibly leading to a blackbody spectrum.

We firstly consider here the case of the simulated observation of a not distorted spectrum, that represents a good test of the possible improvements of an instrument like DIMES, because the limits on $\Delta\epsilon/\epsilon_i$ at relevant redshifts can be directly compared to those obtained with FIRAS data alone. For simplicity, we consider the case of a single energy injection possibly occurred in the cosmic thermal history. The comparison is shown in Fig. 6. As evident, the constraints on $\Delta\epsilon/\epsilon_i$ can be improved by a factor $\sim 10 - 50$ for processes possibly occurred in a wide range of cosmic epochs, corresponding to about a decade in redshift at z about 10^6 . Of course, large energy injections are still possible at very early epochs close to the thermalization redshift, when primordial nucleosynthesis set the ultimately constraints on energy injections in the cosmic radiation field. For late dissipations, FIRAS data mainly constrain $\Delta\epsilon/\epsilon_i$.

As a further example, we consider the constraints on the energy injections at $z_h \geq z_1$ ($y_h \geq 5$) in the case of a fit with a single energy injection to simulated observations of a spectrum distorted at $y_h = 5$ with 5×10^{-6} . As shown by the high redshift tails of the curves of Fig. 3, in this case the constraints on the thermal history of the Universe would be completely different from those derived in the case in which distortions are not detected (Fig. 6). A firm detection of early energy injections would be clearly possible with the considered experimental performances and the constraints on the energy possibly injected at $z > z_1$ could be directly derived from such kind of future CMB spectrum data. In addition, Fig. 6 shows that, contrarily to the case of the current observational status, the constraints on early energy exchanges based on future high accuracy long wavelength measures are no longer appreciably relaxed by assuming that a late process could be also occurred.

6 ENERGY INJECTIONS ABOVE “STANDARD” FIRAS LIMITS AND CHECK OF FIRAS CALIBRATION

In the previous sections, we considered simulated data with a Planckian spectrum or with distortions compatible with the limits derived from FIRAS data calibrated according to Mather et al. 1999. On the other hand, a recent analysis of FIRAS calibration (referred here as “revised”) by Battistelli et al. 2000 suggests a frequency dependence of the FIRAS main calibrator emissivity. The FIRAS data recalibrated according to their “favourite” calibration emissivity law (R-FIRAS data in what follows) indicate the existence of deviations from a Planckian shape or at least a significant relaxation of the constraints on them. Salvaterra & Burigana 2002 discussed the main implications of this analysis. Although it seems quite difficult to fully explain from a physical point of view the R-FIRAS data, two classes of phenomenological models may fit them: in the first one the main contribution derives from an intrinsic CMB spectral distortion with $\Delta\epsilon/\epsilon_i \simeq \text{few} \times 10^{-4}$ occurring at early/intermediate epochs; the second one involves a millimetric component possibly due to cold dust emission, described by a modified blackbody spectrum, added to a CMB blackbody spectrum at a temperature of $\simeq 4$ mK below FIRAS temperature scale of 2.725 K. Fig. 7 shows as these models, very similar at millimeter wavelengths, predict significant differences at centimeter and decimeter wavelengths.

In this section we carefully discuss the capabilities of forthcoming and future CMB spectrum measures at long wavelengths to discriminate between these two different FIRAS calibrations and, in the case of the calibration by Battistelli et al. 2000, to distinguish between the two above scenarios.

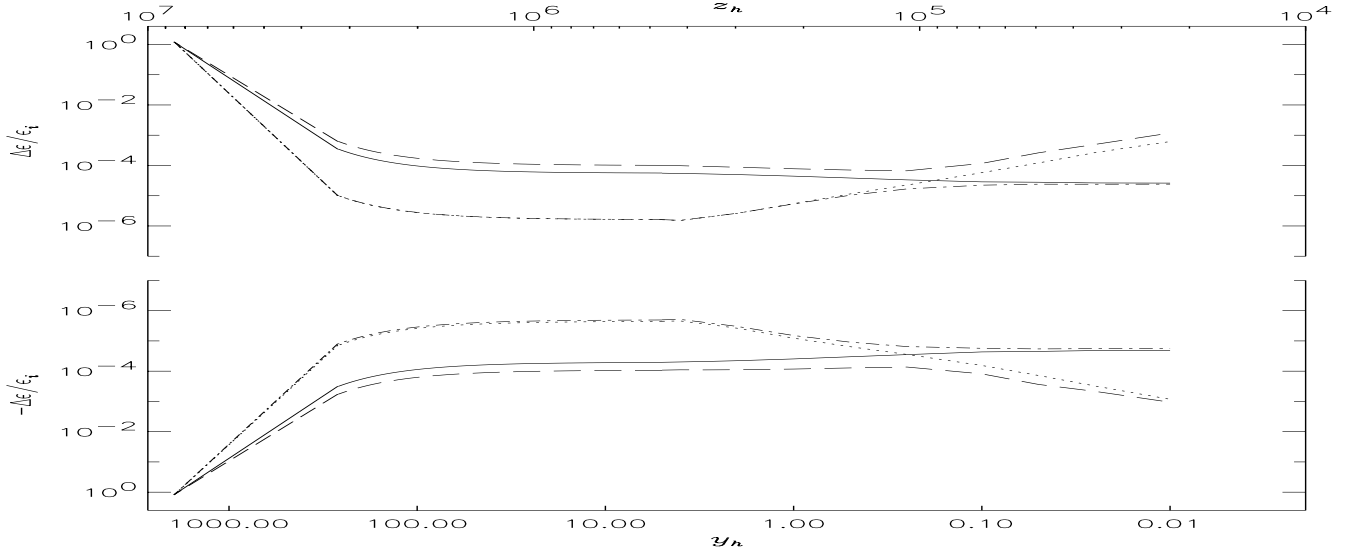


Figure 6. Constraints on the energy exchanges derived from current measures, FIRAS and long wavelength data (solid lines and long dashes; in practice FIRAS data alone set the current constraints, see Salvaterra & Burigana 2002) and from FIRAS data jointed to the simulated data set D-BB (dash-dotted lines and dots). In both cases, the pairs of lines with the more stringent constraints refer to the case in which a single energy exchange is considered, while the others refer to the case of the joint analysis of early/intermediate and late processes.

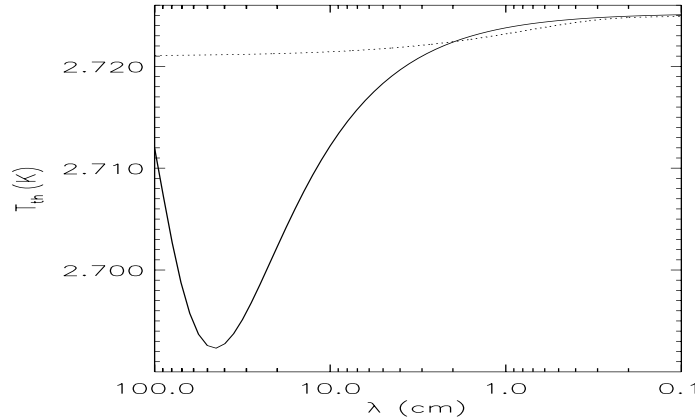


Figure 7. The CMB spectrum as would be observed today (here expressed in terms of equivalent thermodynamic temperature) in the case an early distortion occurring at $y_h = 5$ with $\Delta\epsilon/\epsilon_i = 2 \times 10^{-4}$ (solid line) and in the case of a sum of a pure blackbody spectrum plus a modified blackbody spectrum, representative of typical dust emission, with the parameters of Table 14 of Salvaterra & Burigana 2002 (dots), two models that fit the FIRAS data as recalibrated by Battistelli et al. 2000. Note that these two models, very similar at $\lambda \gtrsim 1$ cm, differ of \simeq some mK – 30 mK at $\lambda \sim$ some cm – some dm.

6.1 Ruling out the “revised” FIRAS calibration

In the case in which the FIRAS calibration by Mather et al. 1999 is substantially correct, and therefore that revised by Battistelli et al. 2000 is wrong, the CMB spectrum is expected to show an essentially Planckian shape also at $\lambda \gtrsim 1$ cm. To test the capabilities of forthcoming and future CMB spectrum experiments to rule out the “revised” calibration we fit simulated observations of a Planckian spectrum at $\lambda \gtrsim 1$ cm generated as described in section 3.1 added to the R-FIRAS data set in terms of a single energy exchange process and of a combination of two processes at different cosmic times. We consider long wavelength data simulated assuming different values of T_0 , at steps of 0.1 mK within the FIRAS temperature scale range, in order to reach the best compromise between them and the non-flat R-FIRAS temperature data. The first five rows of Table 1 summarize our results in the case of a DIMES-like experiment assuming $T_0 \simeq 2.7248$ K, the case in which we find the best agreement. For comparison, we report in the last three rows of Table 1 the results obtained by considering the

$(\Delta\epsilon/\epsilon_i)/10^{-6}$			$\chi^2/\text{d.o.f.}$
$y_h = 5$	$y_h = 1.5$	$y_h \ll 1$	
1.75 ± 1.81			2.401
	4.66 ± 3.81		2.357
		62.37 ± 21.02	1.784
-0.06 ± 1.93		62.61 ± 22.31	1.819
	1.22 ± 4.17	62.10 ± 22.96	1.819
201.5 ± 53.2			1.248
		60.7 ± 23.0	1.906
278.3 ± 96.6		-39.9 ± 41.8	1.194

Table 1. Results of the fit to the R-FIRAS data combined (first five rows) or not (last three rows) with long wavelength data with a sensitivity of a DIMES-like experiment and simulated according to a Planckian shape at $T_0 = 2.7248$ K (first 5 rows) in terms of a single or two dissipation processes at different epochs (fits to two or three parameters: T_0 and one or two values of $\Delta\epsilon/\epsilon_i$). See also the text.

R-FIRAS data alone (Salvaterra & Burigana 2002). As evident from the significant increase of the $\chi^2/\text{d.o.f.}$, long wavelength measures indicating a CMB Planckian shape are not compatible with the FIRAS data calibrated according to Battistelli et al. 2000. Similar analyses carried out in the case of simulated long wavelength Planckian data with the sensitivity of forthcoming, or improved, ground and balloon experiments (data sets G&B1-BB and G&B2-BB) show values of $\chi^2/\text{d.o.f.}$ close to 1.1 – 1.3 (similar to those obtained considering R-FIRAS data alone), when the epoch (or the epochs) and the energy exchange (exchanges) of the dissipation process (processes) is (are) properly chosen.

We then conclude that a CMB spectrum experiment at long wavelengths designed to rule out the FIRAS calibration as revised by Battistelli et al. 2002 should have a sensitivity comparable to that of a DIMES-like experiment.

6.2 Ruling out the “standard” FIRAS results

In the case in which the FIRAS calibration revised by Battistelli et al. 2000 is substantially correct, and therefore that by Mather et al. 1999 is wrong, the CMB spectrum is expected to show deviations from the Planckian shape at $\lambda \gtrsim 1$ cm, as shown in Fig. 7. To test the capabilities of forthcoming and future CMB spectrum experiments to rule out the “standard” FIRAS calibration we consider simulated observations of spectra distorted by an early energy injection or by a significant cold dust contribution, able to account for the FIRAS calibration by Battistelli et al. 2000. Of course, this analysis is useful also to test the capability of future experiments to cross-check the “standard” FIRAS results, independently of the FIRAS calibration revision by Battistelli et al. 2000.

Firstly, we consider the case of long wavelength data simulated according to an early, BE-like distortion occurring at $y_h = 5$ with $\Delta\epsilon/\epsilon_i = 2 \times 10^{-4}$. We exploit three sets of data, the first two with the sensitivities described in section 4.1 (G&B1-BE and G&B2-BE) and the third with the sensitivity of a DIMES-like experiment (D-BE). We consider these data separately and combined with the FIRAS data calibrated according to Mather et al. 1999 and to Battistelli et al. 2000. The result is reported in Table 2.

As evident, measures with sensitivities similar to those of the data set G&B1-BE (see rows 1 – 3 of Table 2) are not able to recognize the inconsistency between the Planckian shape of the “standard” FIRAS data and the long wavelength data, assumed distorted. Also, they can not clearly support the “revised” FIRAS calibration.

On the contrary, with the very high sensitivity of a DIMES-like experiment (see rows 7 – 9 of Table 2) it could be possible to accurately measure the amount of energy dissipated at early cosmic times and accurately cross-check the FIRAS calibration.

Finally, it may be interesting to note that an improvement by a factor ~ 10 of the sensitivity with respect to that of forthcoming ground experiments (as in the case of the data set G&B2-BE; see rows 4 – 6 of Table 2) could provide a significant, although not fully exhaustive, independent test of the FIRAS calibration.

As a second test, we consider the case of long wavelength data simulated according to a Planckian shape plus the contribution from a modified blackbody emission described by the parameters of Table 14 of Salvaterra & Burigana 2002 combined to “standard” FIRAS data at $\lambda \lesssim 1$ cm. We exploit three sets of data, the first two with the sensitivities described in section 4.1 (G&B1-BB/D and G&B2-BB/D) and the third with the sensitivity of a DIMES-like experiment (D-BB/D), and fit them in terms of a pure Planckian spectrum (fits on T_0). The result is reported in Table 3.

As evident, with the very high sensitivity of a DIMES-like experiment it could be possible to probe the disagreement between the long wavelength region of the CMB spectrum and the subcentimetric FIRAS data when calibrated according to Mather et al. 1999. The next ground and balloon experiment do not have enough sensitivity, while a significant, although not fully exhaustive, independent test could be obtained by improving their sensitivities by a factor ~ 10 .

Data set	$(\Delta\epsilon/\epsilon_i)/10^{-4}$	$\chi^2/\text{d.o.f.}$
G&B1-BE	1.64 ± 9.96	0.693
G&B1-BE + FIRAS	0.04 ± 0.53	0.917
G&B1-BE + R-FIRAS	2.01 ± 0.53	1.107
G&B2-BE	1.96 ± 0.99	0.693
G&B2-BE + FIRAS	0.83 ± 0.41	1.301
G&B2-BE + R-FIRAS	1.98 ± 0.41	1.108
D-BE	1.99 ± 0.03	1.056
^(a) D-BE + FIRAS	1.99 ± 0.02	2.041
D-BE + R-FIRAS	1.98 ± 0.02	1.215

Table 2. Results of fits to long wavelength data at different sensitivities simulating the observation of an early energy injection occurring at $y_h = 5$ with $\Delta\epsilon/\epsilon_i = 2 \times 10^{-4}$ combined to the FIRAS data (rows 2, 5, 8), the R-FIRAS data (rows 3, 6, 9) or alone (rows 1, 4, 7). Note that the $\chi^2/\text{d.o.f.}$ of a BE-like spectrum with $\Delta\epsilon/\epsilon_i = 2 \times 10^{-4}$ compared to the “standard” FIRAS data alone is $\simeq 2.177$ (fits to two parameters: T_0 and $\Delta\epsilon/\epsilon_i$; errors at 95 per cent CL). See also the text. ^(a) As generalization of this test, we verified that for a wide range of y_h (between $y_h = 5$ and $y_h \ll 1$) the FIRAS data are not compatible with long wavelength data simulated assuming distortions with $\Delta\epsilon/\epsilon_i = 2 \times 10^{-4}$ and observed with the sensitivity of a DIMES-like experiment, since the large $\chi^2/\text{d.o.f.}$ values found even in the most favourite cases in which the dissipation epoch is assumed known.

Data set	$\chi^2/\text{d.o.f.}$
G&B1-BB/D + FIRAS	0.981
G&B2-BB/D + FIRAS	1.325
D-BB/D + FIRAS	91.10

Table 3. Results of fits to long wavelength data at different sensitivities simulating the observation of a Planckian spectrum plus a contribution from a modified blackbody spectrum described by the parameters of Table 14 of Salvaterra & Burigana 2002 combined to FIRAS data which show a Planckian shape (fits on T_0 assuming a pure blackbody spectrum). Note how the different experimental sensitivity allows or not to test the disagreement between the spectral regions at λ longer or shorter than 1 cm. See also the text.

6.3 Discriminating from different scenarios for the “revised” FIRAS calibration

As discussed in sections 6.1 and 6.2, accurate long wavelength measures could provide independent cross-checks of FIRAS calibration, a DIMES-like experiment being in principle able to firmly rule out the “revised” FIRAS calibration as well as the “standard” one. In the latter case, it is interesting to understand the experimental requirements to discriminate between different scenarios to account for the “revised” FIRAS calibration.

To address this point we consider two representative tests: in the first case we assume an energy injection occurred at early times and try to explain the resulting spectrum in terms of a CMB Planckian spectrum plus a relevant millimetric astrophysical foreground, in the second one we assume a CMB Planckian spectrum plus a relevant millimetric astrophysical foreground and try to explain the resulting spectrum in terms of an early energy injection.

The results of the first test are summarized in Table 4 for our three cases with different long wavelength sensitivities. In this case we re-add (in terms of antenna temperature) the isotropic component (F96) found by Fixsen et al. 1996 (see also section 7 of Burigana & Salvaterra 2002) to the monopole data and consider the simulated long wavelength data combined or not to the R-FIRAS data.

As evident from the very large values the $\chi^2/\text{d.o.f.}$, a DIMES-like experiment could firmly rule out the model involving a relevant millimetric component described by a modified blackbody to account for the “revised” FIRAS calibration, both considered alone and in combination with the R-FIRAS data, so supporting the possibility of a relevant early energy injection to account for the “revised” FIRAS calibration. Again, next ground and balloon experiments do not have enough sensitivity, while an improvement by a factor ~ 10 of their sensitivity may point out the difficulty of a cold dust model in jointly explaining long and short wavelength data.

The results of the second test are summarized in Table 5, again for our three cases with different long wavelength sensitivities.

As evident from the very large $\chi^2/\text{d.o.f.}$, a DIMES-like experiment could firmly rule out the model involving an early energy injection even allowing for a proper adjustment of the value of $\Delta\epsilon/\epsilon_i$, so supporting the model involving a significant millimetric contribution to account for the “revised” FIRAS calibration, while much less accurate experiments do not provide robust answers.

Data set	$\chi^2/\text{d.o.f.}$
G&B1-BE/F96	0.636
G&B1-BE/F96 + R-FIRAS	0.885
G&B2-BE/F96	1.705
G&B2-BE/F96 + R-FIRAS	1.107
D-BE/F96	3231
D-BE/F96 + R-FIRAS	499.3

Table 4. Results of fits to long wavelength data at different sensitivities simulating the observation of an early energy injection occurred at $y_h = 5$ with $\Delta\epsilon/\epsilon_i = 2 \times 10^{-4}$ combined or not to R-FIRAS data (the isotropic foreground F96 is re-added). The fit model includes the two component astrophysical monopole of Table 14 of Salvaterra & Burigana 2002 leaving only T_0 as a free parameter. A DIMES-like experiment could clearly rule out the model involving a relevant millimetric component described by a modified blackbody to account for the “revised” FIRAS calibration, while forthcoming ground experiments do not have enough sensitivity. See also the text.

Data set	$(\Delta\epsilon/\epsilon_i)/10^{-4}$	$\chi^2/\text{d.o.f.}$
G&B1-BB/D	3.41 ± 10.18	1.042
G&B2-BB/D	0.57 ± 0.99	1.108
D-BB/D	0.28 ± 0.03	63.09

Table 5. Results of fits to long wavelength data at different sensitivities simulating the observation of a Planckian spectrum plus a modified blackbody according to Table 14 of Salvaterra & Burigana 2002 in terms of an early spectral distortion occurring at $y_h = 5$ (fits to T_0 and $\Delta\epsilon/\epsilon_i$; errors at 95 per cent CL). A DIMES-like experiment could clearly rule out the model involving an early distortion to account for the “revised” FIRAS calibration. See also the text.

7 FREE-FREE DISTORTIONS

Long wavelength measures are particularly sensitive to the free-free distortion due to its well known dependence on the frequency

$$\frac{T_{th} - T_0\phi_i}{T_0} \simeq \frac{y_B}{x^2}, \quad (6)$$

where ϕ_i is the ratio between the electron and radiation temperature before the beginning of the dissipation process, y_B is the so called free-free distortion parameter (Burigana et al. 1995), and T_{th} is the (frequency dependent) equivalent thermodynamic temperature. The current constraints on the $|y_B|$ depend on the particular set of measures included in the analysis and typically range between $\sim \text{few} \times 10^{-5}$ and $\sim 10^{-4}$ at 95 per cent CL (Salvaterra & Burigana 2002).

In Table 6 we report the best fit values of y_B with the errors at 95 per cent CL and the values of $\chi^2/\text{d.o.f.}$ for different data sets simulated as described in section 3.1 assuming, within the quoted errors, a Planckian spectrum at a temperature of 2.725 K, combined or not with FIRAS data calibrated according to Mather et al. 1999.

As evident, future long wavelength measures can significantly improve the current observational status: constraints on (or detection of) y_B at the (accuracy) level of $\sim 1 - 2 \times 10^{-5}$ can be reached by forthcoming experiments, while improving the sensitivity up to that of a DIMES-like experiment will allow to measure y_b with an accuracy up to about 10^{-7} (errors at 95 per cent CL).

Data set	y_B	$\chi^2/\text{d.o.f.}$
G&B1-BB	$(0.48 \pm 1.38) \times 10^{-5}$	1.027
G&B1-BB + FIRAS	$(0.46 \pm 1.35) \times 10^{-5}$	0.977
G&B2-BB	$(0.48 \pm 1.37) \times 10^{-6}$	1.027
G&B2-BB + FIRAS	$(0.42 \pm 1.36) \times 10^{-6}$	0.979
D-BB	$(0.05 \pm 1.05) \times 10^{-7}$	1.173
D-BB + FIRAS	$(-0.23 \pm 0.88) \times 10^{-7}$	0.976

Table 6. Sensitivity of future long wavelength experiments to the measure of the free-free distortion parameter y_B (errors at 95 per cent CL). See also the text.

8 EXPERIMENTAL REQUIREMENTS FOR A BARYON DENSITY EVALUATION

For distortions at relatively high redshifts ($y_h \gtrsim 1$), the value of $\hat{\Omega}_b$ can be simply determined by the knowledge of the frequency position of the minimum of the CMB absolute temperature:

$$\lambda_{m,BE} \simeq 41.56 \left(\frac{\hat{\Omega}_b}{0.05} \right)^{-2/3} \text{ cm}. \quad (7)$$

This opportunity is very powerful in principle, since the dependence of $\lambda_{m,BE}$ on $\hat{\Omega}_b$ is determined only by the well known physics of the radiation processes in an expanding Universe during the radiation dominated era.

For dissipations at $y_h \gtrsim 5$, the amplitude of this temperature decrement is

$$\Delta T_m \simeq 1.17 \times 10^{-3} \left(\frac{\mu_0}{10^{-5}} \right) \left(\frac{T_0}{2.725 \text{ K}} \right) \left(\frac{\hat{\Omega}_b}{0.05} \right)^{-2/3} \text{ K}, \quad (8)$$

where μ_0 is the chemical potential at the redshift z_1 corresponding to $y_h = 5$.

Eq. (7) gives the range of wavelengths to observe for a firm evaluation of $\hat{\Omega}_b$. As example, for $\hat{\Omega}_b = 0.05$ we need to accurately measure the CMB absolute temperature up to wavelengths of about 50 cm, clearly out from the DIMES range. Ground and ballon experiments are currently planned to reach these wavelengths. Moreover, the amplitude of the maximum dip of the brightness temperature for the energy dissipations at $y_h \gtrsim 5$, see Eq. (8), turns to be at the mK level for $\hat{\Omega}_b \sim 0.05$ and distortions within the FIRAS limits; Burigana et al. 1991a shown that it is about 3 times smaller for energy injections at $y_h \simeq 1$. Experiments designed to estimate $\hat{\Omega}_b$ through the measure of $\lambda_{m,BE}$ should then have a sensitivity level of ~ 1 mK or better.

For sake of illustration, we consider the simulated observation of a spectrum distorted at $y_h = 5$ with $\Delta\epsilon/\epsilon_i = 2 \times 10^{-5}$ (or $\Delta\epsilon/\epsilon_i = 2 \times 10^{-4}$, as suggested by the “revised” FIRAS data) in a $\hat{\Omega}_b = 0.05$ Universe through a very precise experiment extended up to $\lambda \sim 70$ cm. More precisely, we consider the DIMES channels combined to measures at 73.5, 49.1, 36.6, 21.3, 12 and 6.3 cm as those proposed for the space experiment LOBO dedicated to measure the CMB spectrum at very low frequencies (0.408 – 4.75 GHz; see Sironi et al. 1995, Pagana & Villa 1996), but we assume a much better sensitivity, $\simeq 0.1$ mK, comparable to that of the DIMES-like experiment, (or $\simeq 1$ mK). Again, we generate the simulated data as described in section 2.3. The fit to these simulated data by assuming to know the dissipation epoch shows that it would be possible to accurately determine both the amount of injected energy and the baryon density. We recover $\Delta\epsilon/\epsilon_i = (2.11 \pm 0.14) \times 10^{-5}$ (or $\Delta\epsilon/\epsilon_i = (2.11 \pm 0.14) \times 10^{-4}$) and $\hat{\Omega}_b = 0.053 \pm 0.004$ (errors at 95 per cent CL).

Unfortunately, experiments at decimeter wavelengths with a sensitivity of ~ 1 mK or better, although very informative in principle, seem to be very far from current possibilities.

9 CONCLUSIONS

We have studied the implications of possible future observations of the CMB absolute temperature at $\lambda \gtrsim 1$ cm, where both ground, balloon and space experiments are currently under study to complement the accurate FIRAS data at $\lambda \lesssim 1$ cm.

Our analysis shows that future measures from ground and balloon will not be able to significantly improve the constraints on energy exchanges in the primeval plasma already provided by the FIRAS data. Even observations with a sensitivity better by a factor 10 with respect to the realistic performances of the next experiments at different centimeter and decimeter wavelengths can not significantly improve this conclusion.

Thus, we have studied the impact of very high quality data, such those that could be in principle reached with a space experiment. For this analysis, we referred to the DIMES experiment (Kogut 1996), submitted to the NASA in 1995, planned to measure the CMB absolute temperature at $\lambda \sim 0.5 - 15$ cm with a sensitivity of $\simeq 0.1$ mK, close to that of FIRAS.

We have demonstrated that these data would represent a substantial improvement for our knowledge of energy dissipation processes at intermediate and high redshifts ($y_h \gtrsim 1$).

Dissipation processes at $y_h \simeq 5$ could be accurately constrained and possibly firmly detected even for very small amounts of the injected energy ($\Delta\epsilon/\epsilon_i \sim 2 \times 10^{-6}$). For these early dissipation processes it would be possible to estimate also the energy injection epoch. Distortions at intermediate redshifts ($y_h \sim 1.5$) could be also firmly detected, although in this case interesting information on the heating epoch can be derived only for energy injections, $\Delta\epsilon/\epsilon_i$, larger than about 10^{-5} .

On the contrary, by considering the case of a single energy exchange in the thermal history of the Universe, for late processes ($y_h \lesssim 0.1$) a such kind of experiment can not substantially improve the limits based on the FIRAS data at $\lambda \lesssim 1$ cm, which would still set the constraints on $\Delta\epsilon/\epsilon_i$ at late epochs.

By the jointed analysis of two dissipation processes occurring at different epochs, we demonstrated that the sensitivity and frequency coverage of a DIMES-like experiment would allow to accurately recover the amount of energy exchanged in the

primeval plasma at early and intermediate redshifts, and possibly the corresponding epoch, even in presence of a possible late distortion. Even in this case, the constraints on $\Delta\epsilon/\epsilon_i$ can be improved by a factor $\simeq 10 - 50$ for processes possibly occurred in a wide range of cosmic epochs, corresponding to about one–two decades in redshift at z about 10^6 , while the constraints on the energy possibly dissipated at late epochs can be also improved by a factor $\simeq 2$, because the rough compensation between the distortion effects at millimetric wavelengths from an early and a late process with opposite signs becomes much less relevant in presence of very accurate long wavelength data.

In addition, accurate long wavelength measures can provide an independent cross-check of the FIRAS calibration: a DIMES-like experiment could accurately distinguish between the FIRAS calibrations by Mather et al. 1999 and by Battistelli et al. 2000 and in this second case could discriminate between different scenarios to account for it. Interesting, although not fully exhaustive, indications on this aspect could be also obtained by improving the sensitivity of the next ground and balloon experiments by a factor ~ 10 . Further, we have shown that a possible accurate observation of spectral distortions at $\lambda > 1$ cm compatible with relatively large energy injections, compared to the “standard” FIRAS limits, can not be consistently reconciled with the FIRAS data, at least for the class of distortion considered here. In this observational scenario, “exotic” models for spectral distortions should be carefully considered.

We have shown that future long wavelength measures can significantly improve the current observational status of the free-free distortion: constraints on (or detection of) y_B at the (accuracy) level of $\sim 1 - 2 \times 10^{-5}$ can be reached by forthcoming experiments, while improving the sensitivity up to that of a DIMES-like experiment will allow to measure y_b with an accuracy up to about 10^{-7} (errors at 95 per cent CL).

Of course, not only a very good sensitivity, but also an extreme control of the all systematical effects and, in particular, of the frequency calibration is crucial to reach these goals.

Finally, a DIMES-like experiment will be able to provide indicative independent estimates of the baryon density: the product $\Omega_b H_0^2$ can be recovered within a factor $\sim 2 - 5$ even in the case of (very small) early distortions with $\Delta\epsilon/\epsilon_i \sim (5 - 2) \times 10^{-6}$. On the other hand, for $\Omega_b (H_0/50)^2 \lesssim 0.2$, an independent baryon density determination with an accuracy at \sim per cent level, comparable to that achievable with CMB anisotropy experiments, would require an accuracy of ~ 1 mK or better in the measure of possible early distortions but up to a wavelength from $\sim \text{few} \times \text{dm}$ to ~ 7 dm, according to the baryon density value.

ACKNOWLEDGEMENTS

It is a pleasure to thank M. Bersanelli, N. Mandolesi, C. Macculi, G. Palumbo, and G. Sironi for useful discussions on CMB spectrum observations. C.B. warmly thank L. Danese and G. De Zotti for numberless conversations on theoretical aspects of CMB spectral distortions.

REFERENCES

- Battistelli E.S., Fulcoli V., Macculi C. 2000, *New Astronomy*, 5, 77
- Burigana C., Danese L., De Zotti G. 1991a, *A&A*, 246, 59
- Burigana C., De Zotti G., Danese L. 1991b, *ApJ*, 379, 1
- Burigana C., De Zotti G., Danese L. 1995, *A&A*, 303, 323
- Burigana C. & Salvaterra R. 2000, *Int. Rep. ITeSRE/CNR 291/2000*, August
- Danese L. & Burigana C. 1993, in: “Present and Future of the Cosmic Microwave Background”, *Lecture in Physics*, Vol. 429, eds. J.L. Sanz, E. Martinez-Gonzales, L. Cayon, Springer Verlag, Heidelberg (FRG), p. 28
- Danese L. & De Zotti G. 1977, *Riv. Nuovo Cimento*, 7, 277
- Fixsen D.J. et al. 1994, *ApJ*, 420, 457
- Fixsen D.J. et al. 1996, *ApJ*, 473, 576
- Kogut A. 1996, “Diffuse Microwave Emission Survey”, in the *Proceedings from XVI Moriond Astrophysics meeting held March March 16-23 in Les Arcs, France*, astro-ph/9607100
- Kompaneets A.S. 1956, *Zh. Eksp. Teor. Fiz.*, 31, 876 [*Sov. Phys. JEPT*, 4, 730, (1957)]
- Mather J.C., Fixsen D.J., Shafer R.A., Mosier C., Wilkinson, D.T. 1999, *ApJ*, 512, 511
- Nordberg H.P. & Smoot G.F. 1998, astro-ph/9805123
- Pagana E., Villa F., 1996, “The LOBO Satellite Mission: Feasibility Study and Preliminary cost evaluation”, *Int. Rep. C.I.F.S. - 1996*
- Press W.H., Teukolsky S.A., Vetterling W.T., Flannery B.P. 1992, “Numerical Recipes in Fortran”, second edition, Cambridge University Press, USA
- Salvaterra R. & Burigana C. 2000, *Int. Rep. ITeSRE/CNR 270/2000*, March, astro-ph/0206350
- Salvaterra R. & Burigana C. 2002, *MNRAS*, 336, 592
- Sironi G., Bonelli G., Dall’Oglio G., Pagana E., De Angeli S., Perelli M., 1995, *Astroph. Lett. Comm.*, 32, 31
- Staggs S.T., Jarosik N.C., Meyer S.S., Wilkinson D.T. 1996, *ApJ*, 473, L1